Title:

Solid/liquid- and vapor-phase interactions between cellulose- and lignin-derived pyrolysis products

Authors and affiliation:

Takashi Hosoya, Haruo Kawamoto*, Shiro Saka

* Corresponding author: Tal/ Fax: +81-75-753-4737

Email address: kawamoto@energy.kyoto-u.ac.jp (H. Kawamoto)

Full postal address of the person to whom proofs are to be sent:

Graduate School of Energy Science, Kyoto University

Yoshida-honmachi, Sakyo-ku, Kyoto 606-8501, Japan

Abstract:

Solid/liquid- and vapor-phase interactions between cellulose- and lignin (Japanese cedar milled wood lignin)-derived pyrolysis products were studied under the conditions of N_2/ 600^{o}C/ 40-80s. A dual-space closed ampoule reactor was used to eliminate the solid/liquid-phase interactions, and careful comparison of the resulting data with those of the pyrolysis of the mixed samples gave some insights into the solid/liquid- and vapor-phase interactions separately. With the solid/liquid-phase interactions, the tar yields from both cellulose and lignin increased with the decreasing yields of the char fractions in a short pyrolysis time of 40s (primary pyrolysis stage). Most of the identified tar components from cellulose and lignin increased in their yields. The vapor-phase interactions were significant at a longer pyrolysis time of 80s (secondary reaction stage) when the methoxyl groups of the lignin-derived volatiles were cleaved homolytically. The vapor-phase interactions accelerated the gas formation from the cellulose-derived volatiles with suppressing the vapor-phase carbonization of the lignin-derived volatiles. The yields of methane and catechols from lignin also increased greatly instead of the formation of *o*-cresols. Most of these influences are explained with a proposed interaction mechanism, in which the cellulose-derived volatiles act as H-donors while the lignin-derived volatiles (radicals) act as H-acceptors.

Keywords:

Cellulose; lignin; pyrolysis; gasification; interaction; mechanism; H-donor, H-acceptor.

1. Introduction

Pyrolysis is a fundamental process in wood gasification, because the primary pyrolysis products (volatiles and char) are further gasified to CO, CO_2, H_2, and CH_4 [1,2].

Wood constituent polymers, i.e. polysaccharides (cellulose and hemicellulose) and lignin, are pyrolyzed in different ways [3-22], and this leads to the gasification behaviors which are characteristic for these polymers [21-24]. Wood polysaccharides form anhydrosugars, furans, aldehydes, ketones and carboxylic acids as their primary volatile products [6-13,21,22], while the volatiles from lignin mainly consist of the low molecular weight (MW) aromatic compounds with guaiacyl (4-hydroxy-3-methoxyphenyl)-units in case of softwood lignins [6,7,14-22].

As for the secondary reactions, the polysaccharide-derived volatiles are gasified easily in vapor-phase, while these are converted to the solid carbonized products after condensation around the reactor wall with lower temperature [6,25]. The latter char formation substantially reduces the gasification reactivity [22]. Such different gasification reactivities, which are depending on the phases of the primary products, i.e. vapor- v.s. solid/liquid-phases, have been confirmed for levoglucosan (1,6-anhydro-β-D-glucopyranose), a major volatile product from cellulose [26]. Interestingly, furans, aldehydes, ketones and acids have been identified mainly from the solid/liquid-phase pyrolysis. A radical-induced mechanism has been proposed for vapor-phase gasification of levoglucosan.

On the other hand, the lignin-derived volatiles are much less reactive for gasification [22] and rather converted to *o*-cresols, catechols and phenols along with char formation during volatilization [19,27]. Reactivity of this char formation was much higher than that of the carbohydrate-derived vapors. Two competitive pathways, which include direct homolysis of the O-CH_3 bonds in lignin aromatic rings [27-33] and radical-induced rearrangement of the phenyl methyl ethers [27,30,31], have been proposed for formation of catechols and *o*-cresols, respectively. Hosoya et al. [27] also found that the methoxyl groups were necessary for char formation from lignin-related compounds, and they have proposed a char formation mechanism with an *o*-quinone

methide as a key intermediate, which is formed in the course of phenyl methyl ether rearrangement. Thus, formation of *o*-cresols and secondary char could be competitive.

Interactions may be included between polysaccharide- and lignin-derived primary pyrolysis products. Hosoya et al. [34] reported that thermal polymerization of levoglucosan was inhibited in pyrolysis of a cellulose-lignin mixture. They also reported that levoglucosan was stabilized up to 360°C in aromatic compounds with high π-electron densities, such as guaiacol, a primary product from lignin [35]. This stabilization has been explained with their complexation through CH/π interactions [35]. Secondary char formation of lignin-derived volatiles was also inhibited under the influence of cellulose pyrolysis [34,36]. However, details in their interactions are not fully clarified. Understanding the chemical reactions involved in their interactions will be useful in improving the wood gasification processes.

In this paper, solid/liquid- and vapor-phase interactions between cellulose- and lignin-derived pyrolysis products are described. Based on the results, the interaction mechanisms are discussed at the molecular level.

2. Experimental

2-1 Materials

Cellulose powder (cotton, 200-300 mesh, Toyoroshi co.) was used as a cellulose sample. Milled wood lignin was isolated and purified from Japanese cedar (*Cryptomeria japonica*) wood, a softwood, according to the method described in the literature [37]. Moisture content was determined from the decrease in weight after heating at 105 °C for 24 h (cellulose: 8.3 wt%, milled wood lignin: 5.1 wt%). Both samples did not leave inorganic residues in thermogravimetric analysis up to 600 °C in air (10 °C/ min) with a Shimadzu TGA 50. The milled wood lignin sample contained small amount of sugar: hydrolysable sugar content (wt%) determined with the alditol-acetate method [38]: glucose: 0.6, mannose: 0.3, xylose: 0.7, arabinose: 0.2. These sugar impurities arise from hemicellulose included in this sample. Number average of molecular weight of the milled wood lignin sample was about 5000 as a

polystyrene standard from the GPC analysis.

2-2 Reactors

In pyrolysis of solid materials, two interaction modes are considered, i.e. solid/liquid- and vapor-phase interactions. In order to study these interaction modes, two types of the closed ampoule reactors (Type A and B, Fig. 1) were used in this paper. When a cellulose-lignin mixture is pyrolyzed in the Type B reactor, a simple closed ampoule made of Pyrex glass (internal diameter: 8.0 mm, length: 120 mm, glass thickness: 1.0 mm), the two components are decomposed in contact with each other. On the other hand, such direct contact is eliminated in the Type A reactor which has a small inner sample holder (internal diameter: 2.0 mm, length: 10 mm, glass thickness; 1.0 mm) at the bottom of the ampoule. Thus, careful comparison of the results with these two types of reactors gives some information of solid/liquid- and vapor-phase interactions separately.

2-3 Pyrolysis and product analysis

Cellulose (10 mg) and lignin (5 mg) were used. In the Type A reactor, cellulose and lignin were placed at the bottom of the ampoule and in the inner sample holder, respectively. The same sampling sites were used in pyrolysis of pure cellulose or lignin (control experiment). In the Type B reactor, cellulose, lignin or their mixture was placed at the bottom of the ampoule. The ampoules were closed under nitrogen and heated in a muffle furnace preheated at 600 ^{o}C. After 40 or 80s, the ampoule was immediately taken out and cooled with the flowing air for 1 min and then in cold water for 1 min.

The method for gas sampling and analysis were described elsewhere [22]. After the gas analysis, the ampoule and inner sample holder were extracted with dimethyl sulfoxide (DMSO)-d_6 (1.0 mL) to give a DMSO-d_6-soluble portion. The tarry material and water were extracted in this soluble portion. In this paper, the remaining residue is defined as char. The yield of water was determined from the peak area at 3.4-3.5 ppm in the ^{1}H NMR spectrum of the DMSO-d_6-soluble portion with a

Brucker AC-400 (400MHz) spectrometer. The water yield in this paper is shown after subtracting the amount of water originally included in the cellulose and lignin samples. After adding 10 μL of D_2O to the DMSO-d_6-soluble portion to quench the signals of hydroxyl groups, the ^1H NMR measurement was also conducted to determine the cellulose-derived products and organic acids. The yields of levoglucosan, acetic acid, formic acid, hydroxyacetone, furfural, 5-hydroxymethylfurfural (5-HMF) were determined with the signals at δ 5.1 (C_1-H), δ 1.9 (CH_3), δ 8.3 (aldehyde-H), δ 2.0 (CH_3), δ 9.6 (aldehyde-H) and δ 9.7 ppm (aldehyde-H), respectively, using an internal standard (*p*-dibromobenzene). The yield of glycolaldehyde was determined as the oxime derivatives (*E*- and *Z*-isomers) by ^1H NMR, after oximation with hydroxylamine hydrochloride (2.0 mg) added to the DMSO-d_6 solution. The signals (-HC=N-OH) at δ 7.3 (*E*-isomer) and δ 6.7 ppm (*Z*-isomer) were used for their quantification.

Gas chromatography–mass spectrometry (GC/MS) was conducted with a Hitachi G-7000 gas chromatograph and a Hitachi M9000 mass spectrometer. The lignin-derived products in the tar fractions were determined quantitatively with the GC-MS analysis of the MeOH-soluble portions, which were obtained by extracting the tar fractions with MeOH (1.0 mL), with *p*-dibromobenzene as an internal standard. Chromatographic conditions were: column: Shimadzu CBP-M25-O25 (length: 25 m, diameter: 0.25 mm), injector temperature: 250 °C, column temperature: 40 °C (1 min), 40 → 300 °C (1 → 53 min), 300 °C (53 → 60 min), carrier gas: helium, flow rate: 1.5 ml/min, emission current: 20 μA, ionization time: 2.0 ms. Identification of the products is described in the previous paper [19]. Mass chromatograms (Fig. 2) were used for determination, because the total-ion chromatograms of the pyrolyzates obtained from the co-pyrolysis of lignin with cellulose became complicated.

The amount of tar fraction was calculated by subtracting the weight of the gaseous products (CO, CO_2, H_2 and CH_4), char and water from the weight of the original sample. The char yield was determined from the weight difference of the ampoule after combustion in air at 600 °C for 2 h.

3. Results and discussion

3-1 Gas, tar and char formation behavior

Figure 3 shows the pictures of the reactors (Type A) after pyrolysis (N_2/ 600ºC/ 40 or 80 s) and subsequent tar extraction. In 40 s, the lignin and cellulose samples formed solid carbonized products in the inner sample holder and the bottom of the ampoule, respectively. Secondary char from lignin was also observed around the ampoule reactor wall in 80s as reported in our previous paper [6,22,27]. This secondary char formation was effectively inhibited in co-pyrolysis with cellulose (cellulose: lignin = 2:1, w/w) [34]. Since the solid/liquid-phase interaction is not effective in the Type A reactor, this inhibitory effect arises from the vapor-phase interaction. Similar inhibition of the secondary char formation was observed also in the Type B reactor.

Yields of gas, tar, water and char are summarized in Table 1, as compared with those of pure cellulose or lignin pyrolysis (control experiment). Table 1 also includes the estimated yields in parentheses on the assumption that there are no interactions during pyrolysis. Deviations between experimental and estimated yields indicate interaction between cellulose and lignin.

In 40s, the tar yield increased from 45.7 wt% (estimated) to 55.1 wt% (experimental) with the suppressing formation of char (32.5 to 28.3 wt%) and water (16.7 to 11.6 wt%) in the Type B reactor. The influences in the Type A reactor were comparatively small. The water yields were usually correlated with the char yields, since dehydration is a main process in carbonization. These observed influences suggest that the solid/liquid-phase interaction in the early stage of pyrolysis (primary pyrolysis stage) enhances the tar formation instead of char and water.

Gasification of the primary products proceeded in the period of 40-80s. In cellulose pyrolysis (control), the gas yield increased from 5.0 wt% (40s) to 31.1 wt% (80s) with the decreasing yield of tar from 54.0 wt% (40s) to 29.3 wt% (80s), although the char yields were not so different (40s: 17.7 wt%, 80s: 17.0 wt%). Thus, gasification of the cellulose-derived tar components proceeded in this period. Contrary to this, gas formation from lignin (control experiment) [5.3 wt% (40s) to 10.5 wt%

(80s)] was comparatively small. Such lower gasification reactivity of lignin primary tar is in agreement with the literature [22]. Under the co-pyrolysis conditions, the experimental gas yields (80s) (Type A: 31.4 wt%, Type B: 28.9 wt%) were greater than the estimated one (80s) (24.2 wt%), while the estimated and experimental gas yields in 40s were similar (Type A: 4.7 wt%; Type B: 5.0 wt%, estimated: 5.0 wt%). Accordingly, gas formation in the period of 40-80s (secondary reaction stage) was accelerated in co-pyrolysis.

3-2 Gas and tar components

Yields of the non-condensable gases (CO_2, CO, CH_4 and H_2) are summarized in Table 2. Deviation between experimental and estimated yields is shown as a yield difference value (YD) (Fig. 4), which is defined in this paper as the ratio of experimental yield / estimated yield. From the definition, the YD value > 1.0 indicates the enhanced formation or *vice versa*.

In 40s, major influence was observed on the yield of methane. The methane yields under the co-pyrolysis conditions were much lower than the estimated yields [YD values: 0.55 (Type A) and 0.23 (Type B)]. Although the inhibition mechanism is not clear presently, the O-CH_3 bond homolysis may be inhibited in lignin pyrolysis products formed under the influence of cellulose pyrolysis. From the greater influence in the Type B reactor, this inhibition is more related to the solid/liquid-phase interaction. In a longer pyrolysis time of 80s, formation of all gases, especially methane in the Type A reactor, were accelerated.

Yields of the tar components are summarized in Table 3. Their YD values are also shown in Fig. 5 (for compounds) and Fig. 6 (for compound types). Under the present conditions (control experiments), the listed compounds in Table 3 cover 27.2 wt% (40s) and 25.2 wt% (80s) of the tar fractions from cellulose, and 17.4 wt% (40s) and 21.8 wt% (80s) of the tar fractions from lignin. Other tar components may exist as the compounds with higher molecular masses which could not be identified with GC-MS and ^{1}H NMR analyses as indicated in the previous papers [6,19].

Anhydrosugar, C_2-C_3 carbonyls and furans were identified in the

cellulose-derived tar fractions. As for lignin, all of the GC/MS-detectable products (40s) have the guaiacyl-units, the aromatic nuclei in the original lignin (Table 3). This indicates that the O-CH_3 bond homolysis in vapor-phase is not effective in 40s. This is not consistent with the methane formation (control: 0.67 wt%) in 40s. Homolysis of some O-CH_3 bonds would occur in the higher MW products (undetectable in GC/MS analysis), although the activation mechanism is not clear. As already described, this early stage methane formation is inhibited in co-pyrolysis with cellulose (Table 2, Fig. 4).

Organic acids (formic acid and acetic acid) were identified from both samples, and hence, it is unclear how much of these acids are formed from cellulose and lignin, respectively, under the co-pyrolysis conditions. Accordingly, yields of these acids in co-pyrolysis (shown in Table 3) are based on the amount of cellulose + lignin, while yields of other cellulose- and lignin-derived products are shown based on cellulose and lignin, respectively.

In primary pyrolysis stage (40s), yields of the identified tar components from cellulose and lignin increased under the co-pyrolysis conditions (Type B reactor): cellulose-derived: from 13.5 wt% (control: only cellulose) to 19.8 wt%; lignin-derived: from 4.5 wt% (control: only lignin) to 7.0 wt% (Table 3). YD values of most cellulose- and lignin-derived tar components (except formic acid) were > 1.0 (Figs. 5 and 6). Thus, most of the GC/MS- and ^{1}H NMR-detectable tar components from cellulose and lignin increase in their yields under the co-pyrolysis conditions with the Type B reactor. These results coincide with the enhanced tar formation (45.7 wt% to 55.1 wt%, Table 3). Contrary to this, the yields in the Type A reactor (cellulose-derived: 12.9 wt%, lignin-derived: 5.2 wt%) were not so different from those of the control experiments.

Even in the Type A reactor (40s), tar composition changed. As for cellulose, yield of anhydrosugar (levoglucosan) decreased (YD: 0.80), while yields of C_2-C_3 carbonyls and furans increased (YDs: 1.2 and 1.2, respectively) (Fig. 6). Several researchers have reported that yields of anhydrosugar and C_2-C_3 carbonyls were in trade-off relationship [10,13,39], and these relationships have been explained with two

competitive pathways [10,13]. The lignin-derived volatiles may change the selectivity of these two pathways.

Composition of the side-chain structures of the GC/MS-detectable lignin-derived compounds (40s) changed under the influence of cellulose pyrolysis (Fig. 5). The contents of saturated side-chains (ethyl- and propyl- groups) and >C=O increased instead of >C=C< (Type A reactor). In the Type B reactor, formation of unsubstituted (H-) and methyl guaiacols was preferable to other side-chain structures. Unlike the Type A reactor, shorter saturated side-chains tend to be formed in the Type B reactor: YD values: propyl- (1.6) > ethyl- (1.2) > methyl- (1.0) > H- (0.80) (Type A); H- (3.9) > methyl- (3.0) > ethyl- (1.5) > propyl- (1.1) (Type B).

In the secondary reaction stage (40-80s), the decreasing rate of the total yield of the identified cellulose-derived tar components increased in co-pyrolysis (control: 13.5 to 6.2 wt%, Type A: 12.9 to 3.7 wt%, Type B: 19.8 to 6.7 wt%, based on cellulose, Table 3). The YD values of all identified products from cellulose decreased in this period [anhydrosugar: 0.80 to 0.69 (1.4 to 1.0), C_2-C_3 carbonyls: 1.2 to 0.45 (1.5 to 1.2), furans: 1.2 to 0.60 (1.9 to 1.3), Type A reactor (figures in parenthesis, Type B reactor)] (Figs. 5 and 6). These results and the observed acceleration of the gas formation (Fig. 4) suggest that gasification of all cellulose-derived tar components listed in Table 3 is enhanced under the influence of lignin pyrolysis.

On the other hand, yields of the GC/MS-detectable lignin-derived products rather increased in 40-80s (control: 4.5 to 5.3 wt%, Type A: 5.2 to 9.5 wt% and Type B: 7.0 to 20.2 wt%, based on lignin, Table 3). This increasing rate was larger in co-pyrolysis: control < Type A < Type B. Accordingly, co-pyrolysis with cellulose, especially pyrolysis of a cellulose-lignin mixture in the Type B reactor, enhanced the formation of low MW products in the secondary reaction stage (40-80s). These low MW products are expected to be formed through cracking of the side-chains of the primary higher MW products as discussed later.

As for the compound-type, GC-detectable guaiacols were completely replaced by catechols, *o*-cresols and phenols in 40-80s. The O-CH_3 bond homolysis to give catechols and the radical-induced rearrangement to *o*-cresols [19,27-33] proceed in this

period. As for the side-chain structure, unsaturated structures (>C=C< and >C=O) disappeared except for *E*-4-(1-propenyl)-2-methylphenol. These structural changes are in agreement with the previous paper [19]. Co-pyrolysis with cellulose changed the tar compositions obtained from these secondary reactions of lignin. Yields of catechols increased substantially (YD values: Type A: 2.5; Type B: 5.5, Figs. 5 and 6), while the yields of *o*-cresols rather decreased (YD values: Type A: 0.53; Type B: 0.94). Consequently, the ratio of catechols / *o*-cresols increased enormously.

3-3 Interaction mechanisms

The major solid/liquid- and vapor-phase interactions observed in this study are summarized in Table 4. Some of these influences are explainable by considering the cellulose- and lignin-derived pyrolysis products as H-donors and H-acceptors, respectively (Figs. 7-9).

In primary pyrolysis of lignin (pathway a in Fig. 7), large parts of the products are produced as radical species. Kawamoto et al. [15,16] have studied the cleavage mechanisms (heterolysis vs. homolysis) of the lignin ether linkages (α- and β-ether types) from the substituent effects on the reactivity, and they concluded that the ether linkages other than the α-ether linkage in phenolic form are cleaved homolytically. Some of the radical species formed by the cleavage of the β-ether linkages (the most abundant linkage-type in lignin) are further converted to the coniferyl alcohol-type products [15-18,20] through the β-scission type reactions. Thus, many of the primary pyrolysis products from lignin have the >C=C< structures. Such >C=C< structures polymerize shortly to form high MW products (pathway b in Fig. 7) [19,40]. Vinyl condensation mechanism is proposed for this polymerization by Nakamura et al. [40]. Phenoxy and alkyl radicals are also involved in this polymerization through radical coupling reactions [40]. Then, cracking of the side-chains (pathway c in Fig. 7) occurs to form low MW radicals which are stabilized as aromatic compounds with saturated alkyl- and H- groups by H-donation from other products [19] (pathway d in Fig. 7). In the course, the aromatic structure is also changed as described in the scheme (Fig. 8).

In the proposed interaction mechanism (Fig. 7), the cellulose-derived products

act as H-donors to the radical species in pathways d and e. Stabilization of the primary radicals by this H-donation in pathway e enhances the formation of low MW aromatic products with saturated alkyl groups, instead of the double bond formation and condensation. Lower composition ratio of the >C=C< structures than the saturated side-chains as observed in co-pyrolysis with the Type A reactor (40s, Fig. 5) support this proposal.

In the presence of the cellulose-derived products, low MW radical species formed through cracking of the side-chains of the high MW products are stabilized as aromatic compounds with saturated alkyl side-chains and –H, instead of the recombination to higher MW products (pathway d). Such interaction is expected to be more effective in solid/liquid-phase, because less volatile condensation products tend to stay in the solid/liquid-phase. Enormously high yields of the low MW products in the Type B reactor (80s, Fig. 5) are explainable with this mechanism.

Influences on the catechols/ *o*-cresols ratio, methane yield and secondary char formation behavior are explained with the proposed mechanisms in Fig.8. Two competitive pathways are known for conversion of the guaiacyl-unit [27,31]. One is direct homolysis of the O-CH_3 bonds to form catechol and methyl radicals which are further stabilized by H-donation from other products as catechols and methane. The other pathway is a radical-induced rearrangement from phenyl-O-CH_3 to phenyl-CH_2-O- structures [30,31]. Finally, this pathway gives *o*-cresols and secondary char via the *o*-quinone methide intermediates [27]. This reaction is initiated from the intramolecular H-abstraction at the methyl hydrogen by phenoxy radical. Consequently, the product selectivity between catechols + methane and *o*-cresols + secondary char is determined by the phenol/ phenoxy radical ratio. In the presence of the cellulose-derived products (H-donors), this ratio moves to the direction where the phenolic form is preferable. Similarly, formation of catechols and methane from their radicals and hydrogenation of the *o*-quinone methides to *o*-cresols would also be more effective.

Although the details of the interactions such as the structures of the H-donors are unclear presently, the influences on lignin pyrolysis are explained with the H-donation

from the cellulose-derived products. From the cellulose side, the lignin-derived radicals abstract hydrogens from the cellulose-derived products. This may enhance the gasification of the primary products in vapor-phase (Fig. 9). As a proof for this proposal, Hosoya et al. [26] have reported that levoglucosan, a major tar component from cellulose, was gasified effectively in vapor-phase through a radical-induced mechanism, although char formation preferably proceeded in solid/liquid-phase. The radical-induced mechanism has been proposed based on the observed isotope effect on inhibition of the gasification by acetaldehyde (a H-donor).

4. Conclusions

Solid/liquid- and vapor-phase interactions were indicated in co-pyrolysis of cellulose and lignin under the conditions of N_2/ 600^{o}C/ 40-80 s. The solid/liquid-phase interaction accelerated the tar formation from both cellulose and lignin, with the reducing char and water formation. On the other hand, the vapor-phase interaction enhanced the gasification of the cellulose-derived volatiles. The catechols and methane yields also increased instead of *o*-cresols and secondary char from lignin. Most of these influences are explained with the actions of the cellulose- and lignin-derived products as the H-donors and the H-acceptors, respectively.

Acknowledgment

This research was supported by a Grant-in-Aid for Scientific Research (C)(2)(No. 16580132, 2004.4-2006.3) and 21st COE program “Establishment of Sustainable Energy System” from Ministry of Education, Culture, Sports, Science and Technology, Japan.

References

[1] T.A. Milne, N. Abatzoglou, R. J. Evance, Biomass Gasifire “Tars”: Their Nature, Formation and Conversion, NREL/ TP-570-25357 (1998) p.1-68.

[2] S. Rapagna, N. Jand, P. U. Foscolo, Intl. J. Hydrogen Energy, 23 (1998) 551.

[3] J. J. M. Órfão, F. J. A. Antunes, J. L. Figueiredo, Fuel 78 (1999) 349.

[4] K. Raveendran., A. Ganesh, K. Khilar, Fuel 75 (1996) 987.

[5] G. Várhegyi, M. J. Antal, Jr., E. Jakab, P. Szabó, J. Anal. Appl. Pyrol. 42 (1997) 73.

[6] T. Hosoya, H. Kawamoto, S. Saka, J. Anal. Appl. Pyrol. 78 (2007) 328.

[7] A. D. Pouwels, J. J. Boon, J. Anal. Appl. Pyrol. 17 (1990) 97.

[8] E.-J. Shin, M. R. Nimlos, R. J. Evans, Fuel 80 (2001), 1697.

[9] A. D. Pouwels, G. B. Eijkel, J. J. Boon, J. Anal. Appl. Pyrol. 14 (1989) 237.

[10] J. Piskorz, D. St. A. G. Radlein, D. S. Scott, J. Anal. Appl. Pyrol. 16 (1989) 127.

[11] F. Shafizadeh, J. Anal. Appl. Pyrol. 3 (1982) 283.

[12] O. Faix, D. Meier, I. Grobe, J. Anal. Appl. Pyrol. 11 (1987) 403.

[13] G. N. Richards, J. Anal. Appl. Pyrol. 10 (1987) 251.

[14] J. R. Obst, J. Wood Chem. Technol. 3 (1983) 377.

[15] H. Kawamoto, T. Nakamura, S. Saka, Holzforsch. 62 (2008) 50.

[16] H. Kawamoto, M. Ryoritani, S. Saka, J. Anal. Appl. Pyrol. 81 (2008) 88.

[17] H. Kawamoto, S. Horigoshi, S. Saka, J. Wood. Sci 53 (2007) 168.

[18] T. Nakamura, H. Kawamoto, S. Saka, J. Anal. Appl. Pyrol. 81 (2008) 173.

[19] T. Hosoya, H. Kawamoto, S. Saka, J. Anal. Appl. Pyrol., 83 (2008) 78.

[20] R. Brežný, V. Mihálov, V. Kváčik Holzforsch. 37 (1983) 199.

[21] R. J. Evans, T. A. Milne, Energy & Fuels 1 (1987) 123.

[22] T. Hosoya, H. Kawamoto, S. Saka, J. Anal. Appl. Pyrol., 83 (2008) 71.

[23] M. J. Antal, Jr, Ind. Eng. Chem. Prod. Res. Dev. 22 (1983) 366.

[24] C. Fushimi, K. Araki, Y. Yamaguchi, A. Tsutsumi, Ind. Eng. Chem. Res. 42 (2003) 3929.

[25] H. Kawamoto, M. Murayama, S. Saka, *J. Wood Sci*. 49 (2003) 469.

[26] T. Hosoya, H. Kawamoto, S. Saka, J. Anal. Appl. Pyrol., 83 (2008) 64.

[27] T. Hosoya, H. Kawamoto, S. Saka, J. Anal. Appl. Pyrol., in press.

[28] R. Ceylan and J. B-son Bredenberg, Fuel 61 (1982) 377.

[29] H. E. Jegers, M. T. Klein, Ind. Eng. Chem. Process Des. Dev. 24 (1985) 173.

[30] A. Vuori, Fuel 65 (1986) 1575.

[31] E. Dorrestijn, P. Mulder, J. Chem. Soc., Perkin Trans. 2 (1999) 777.

[32] R. H. Schlosberg, P. F. Szajowski, G. D. Dupre, J. A. Danik, A. Kurs, T. R. Ashe, W. N. Olmstesd, Fuel 62 (1983) 691.

[33] A. I. Vuori, J. B-son Bredenberg, Ind. Eng. Chem. Res. 26 (1987) 359.

[34] T. Hosoya, H. Kawamoto, S. Saka, J. Anal. Appl. Pyrol. 80 (2007) 118.

[35] T. Hosoya, H. Kawamoto, S. Saka, Carbohydr. Res. 341 (2006) 2293.

[36] T. Hosoya, H. Kawamoto, S. Saka, J. Wood Sci. 53 (2007) 351.

[37] A. Bjorkman, Svensk paperstidn 59 (1956) 477.

[38] L. G. Borchardt, C. V. Piper, Tappi 53 (1970) 257.

[39] G. N. Richards, G. Zheng, J. Anal. Appl. Pyrol. 21 (1987) 133.

[40] T. Nakamura, H. Kawamoto, S. Saka, J. Wood Chem. Technol. 27 (2007) 12

Legend of tables and figures

Table 1 Changes in the fractional composition (wt%, oven-dry basis) in co-pyrolysis of cellulose and lignin (N_2/ 600 ^oC).

Table 2 Yield (wt%, oven-dry basis) of the gaseous products (N_2/ 600 ^oC).

Table 3 Yields (wt%, oven-dry basis) of some identified products from the tar fractions (N_2/600 ^oC).

Table 4 Summary of the influences of the solid/liquid- and vapor-phase interactions on formation of the pyrolysis products from cellulose and lignin (N_2/ 600 ^oC).

Fig. 1 Two-types of the reactors used in this study.

Fig. 2 Total-ion chromatograms and mass chromatograms measured for the MeOH-soluble potions obtained in co-pyrolysis of cellulose and lignin (2:1, w/w) (Type A reactor, N_2/ 600 ^oC).
A: 40 s, B: 80 s.

Fig. 3 Ampoules after pyrolysis and tar extraction (Type A reactor).

Fig. 4 Yield difference values (YDs) (YD: experimental yield/ estimated yield) obtained for the gaseous products in co-pyrolysis of cellulose and lignin (2:1, w/w) (N_2/ 600 ^oC).
[a] Hydrogen was not detected at 40s.

Fig. 5 Yield difference values (YDs) (YD: experimental yield/ estimated yield) obtained for the low MW compounds identified from the tar fractions in co-pyrolysis of cellulose and lignin (2:1, w/w) (N_2/ 600 ^oC).

Fig. 6 Yield difference values (YDs) (YD: experimental yield/ estimated yield) of the types of the products in co-pyrolysis of cellulose and lignin (2:1, w/w) (N_2/ 600 ^oC).
[a] Not detected.

Fig.7 A proposed mechanism for the influences of the cellulose-derived products on the tar formation from lignin.
Bold arrows: enhanced by the cellulose-derived products.

Fig.8 A proposed mechanism for the influences of the cellulose-derived products on the aromatic composition (catechols / *o*-cresols) and the secondary char formation in lignin pyrolysis.
Bold arrows: enhanced by the cellulose-derived products.

Fig.9 A proposed mechanism for acceleration of the cellulose gasification by the lignin-derived products.
Bold arrow: enhanced by the lignin-derived products.

Table 1
Changes in the fractional composition (wt%, oven-dry basis) in co-pyrolysis of cellulose and lignin (N_2/ 600 °C).

	Pyrolysis time [s]	Gas	Water	Tar	Char
Cellulose	40	5.0	23.3	54.0	17.7
Milled wood lignin	40	5.3	3.5	29.0	62.2
Co-pyrolysis[a] (Type A reactor)	40	4.7 (5.0)	15.2 (16.7)	49.1 (45.7)	31.0 (32.5)
Co-pyrolysis[a] (Type B reactor)	40	5.0 (5.0)	11.6 (16.7)	55.1 (45.7)	28.3 (32.5)
Cellulose	80	31.1	22.6	29.3	17.0
Milled wood lignin	80	10.5	11.2	27.2	51.1
Co-pyrolysis[a] (Type A reactor)	80	31.4 (24.2)	15.0 (18.8)	27.1 (28.6)	26.5 (28.4)
Co-pyrolysis[a] (Type B reactor)	80	28.9 (24.2)	12.1 (18.8)	36.0 (28.6)	23.0 (28.4)

Figures in parentheses show the estimated yields from the composition of cellulose and lignin on the assumption that there are no interactions between them.
[a] Cellulose: milled wood lignin = 2:1 (w/w).

Table 2
Yield (wt%, oven-dry basis) of the gaseous products (N_2/ 600 °C).

	Cellulose	Lignin	Co- pyrolysis [a] (Type A reactor)	Co- pyrolysis [a] (Type B reactor)	Cellulose	Lignin	Co- pyrolysis [a] (Type A reactor)	Co- pyrolysis [a] (Type B reactor)
Pyrolysis time (s)	40	40	40	40	80	80	80	80
CO_2	2.8	1.8	2.4	2.6	11	3.6	9.4	9.4
CO	2.2	2.8	2.2	2.4	19	5.1	17	17
CH_4	Trace	0.67	0.12	Trace	1.3	2.2	4.8	2.2
H_2	ND	ND	ND	ND	0.13	0.025	0.11	0.10
Total	5.0	5.3	4.7	5.0	31	11	31	29

[a] Cellulose: milled wood lignin mixture = 2:1 (w/w).

Table 3
Yields (wt%, oven-dry basis) of some identified products from the tar fractions (N_2/600 °C).

	Cellulose	Lignin	Co-pyrolysis[a] (Type A reactor)	Co-pyrolysis[a] (Type B reactor)	Cellulose	Lignin	Co-pyrolysis[a] (Type A reactor)	Co-pyrolysis[a] (Type B reactor)
Pyrolysis time (s)	40	40	40	40	80	80	80	80
Cellulose-derived[b]	**13.5 (24.9)**	—	**12.9**	**19.8**	**6.2 (20.8)**	—	**3.7**	**6.7**
Anhydrosugar	**7.9 (14.6)**	—	**6.3**	**11.0**	**3.6 (12)**	—	**2.5**	**3.6**
Levoglucosan	7.9 (14.6)	—	6.3	11.0	3.6 (12)	—	2.5	3.6
C_2-C_3 carbonyls	**4.6 (8.5)**	—	**5.4**	**6.9**	**2.2 (7.4)**	—	**1.0**	**2.6**
Glycolaldehyde	3.7 (6.9)	—	4.1	5.1	1.2 (4.1)	—	0.60	1.6
Hydroxyacetone	0.86 (1.6)	—	1.3	1.8	0.96 (3.3)	—	0.41	1.0
Furans	**0.99 (1.8)**	—	**1.2**	**1.9**	**0.40 (1.4)**	—	**0.24**	**0.51**
Furfural	0.44 (0.81)	—	0.53	0.61	0.24 (0.82)	—	0.17	0.29
5-HMF	0.55 (1.0)	—	0.66	1.3	0.16 (0.55)	—	0.074	0.22
Cellulose- and lignin-derived[c]	**1.3 (2.3)**	**0.53 (1.8)**	**1.3**	**0.98**	**1.3 (4.4)**	**0.42 (1.6)**	**0.83**	**0.92**
Acids	**1.3 (2.3)**	**0.53 (1.8)**	**1.3**	**0.98**	**1.3 (4.4)**	**0.42 (1.6)**	**0.83**	**0.92**
Formic acid	0.67 (1.2)	0.11 (0.37)	0.53	0.41	0.088 (0.30)	—	Trace	0.062
Acetic acid	0.62 (1.1)	0.42 (1.4)	0.77	0.57	1.2 (4.1)	0.42 (1.6)	0.83	0.86
Lignin-derived[d]	—	**4.5 (15.6)**	**5.2**	**7.0**	—	**5.3 (20.2)**	**9.5**	**20.2**
Guaiacols	—	**4.5 (15.6)**	**5.2**	**7.0**	—	—	—	—
Guaiacol	—	0.20 (0.69)	0.16	0.78	—	—	—	—
4-Methylguaiacol	—	0.27 (0.93)	0.27	0.81	—	—	—	—
4-Ethylguaiacol	—	0.11 (0.38)	0.13	0.17	—	—	—	—
4-Propylguaiacol	—	0.16 (0.55)	0.26	0.18	—	—	—	—
4-Vinylguaiacol	—	0.16 (0.55)	0.11	0.26	—	—	—	—
Eugenol	—	0.076(0.26)	0.068	0.15	—	—	—	—
Z-isoeugenol	—	0.11 (0.38)	0.073	0.15	—	—	—	—
E-isoeugenol	—	0.69 (2.4)	0.59	0.97	—	—	—	—
Vanillin	—	1.6 (5.5)	2.2	2.2	—	—	—	—
Homovanillin	—	0.053(0.18)	0.19	0.12	—	—	—	—
Acetovanillone	—	0.19 (0.66)	0.25	0.27	—	—	—	—
Coniferyl aldehyde	—	0.90 (3.1)	0.92	0.92	—	—	—	—
Catechols	—	—	—	—	—	**3.3 (12.6)**	**8.2**	**18.0**
Pyrocatechol	—	—	—	—	—	1.2 (4.6)	2.4	5.5
4-Methylcatachol	—	—	—	—	—	1.5 (5.8)	4.2	9.3
4-Ethylguaiacol	—	—	—	—	—	0.56 (2.2)	1.6	3.2
***o*-Cresols**	—	—	—	—	—	**1.6 (6.1)**	**0.85**	**1.5**
o-Cresol	—	—	—	—	—	0.44 (1.7)	0.28	0.48
2,4-Xylenol	—	—	—	—	—	0.63 (2.4)	0.30	0.57
4-Ethyl-2-methylphenol	—	—	—	—	—	0.27 (1.0)	0.15	0.32
2-Methyl-4-propylphenol	—	—	—	—	—	0.099(0.38)	0.066	0.056
E-2-Methyl-4-(1-propenyl) phenol	—	—	—	—	—	0.15 (0.58)	0.054	0.054
Other phenols	—	—	—	—	—	**0.40 (1.5)**	**0.44**	**0.74**
Phenol	—	—	—	—	—	0.21 (0.81)	0.23	0.40
p-Cresol	—	—	—	—	—	0.19 (0.73)	0.21	0.34
Total	**14.8 (27.2)**	**5.0 (17.4)**	—	—	**7.5 (25.2)**	**5.7 (21.8)**	—	—

Figures in parentheses show the yields based on the weights of the tar fractions.
[a] Cellulose: milled wood lignin = 2:1, w/w [b] Yields are based on cellulose. [c] Yields are based on cellulose, lignin or cellulose + lignin (in case of co-pyrolysis). [d] Yields are based on lignin.

Table 4
Summary of the influences of the solid/liquid- and vapor-phase interactions on formation of the pyrolysis products from cellulose and lignin (N_2/ 600 °C).

Solid/liquid-phase	
Gas	+/−
CH_4 from lignin	−
Tar	+
From cellulose	+
From lignin	+
Char	−
Vapor-phase	
Gas	+
Gas from cellulose	+
CH_4 from lignin	+
Tar	+/−
From cellulose	−
From lignin	+
Catechols	+
o-Cresols	−
Char	(−)
Secondary char from lignin	−

+: enhanced formation, −: suppressed formation

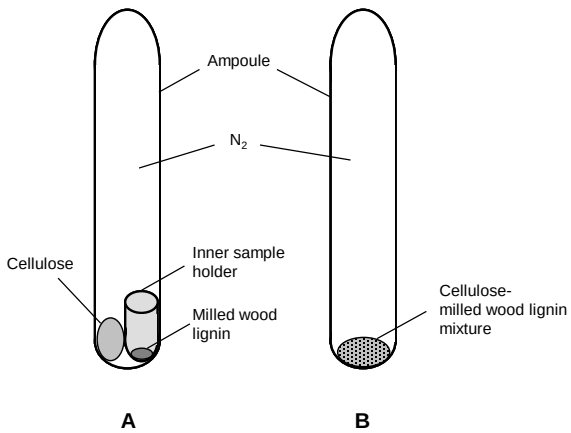

Fig. 1 Two-types of the reactors used in this study.

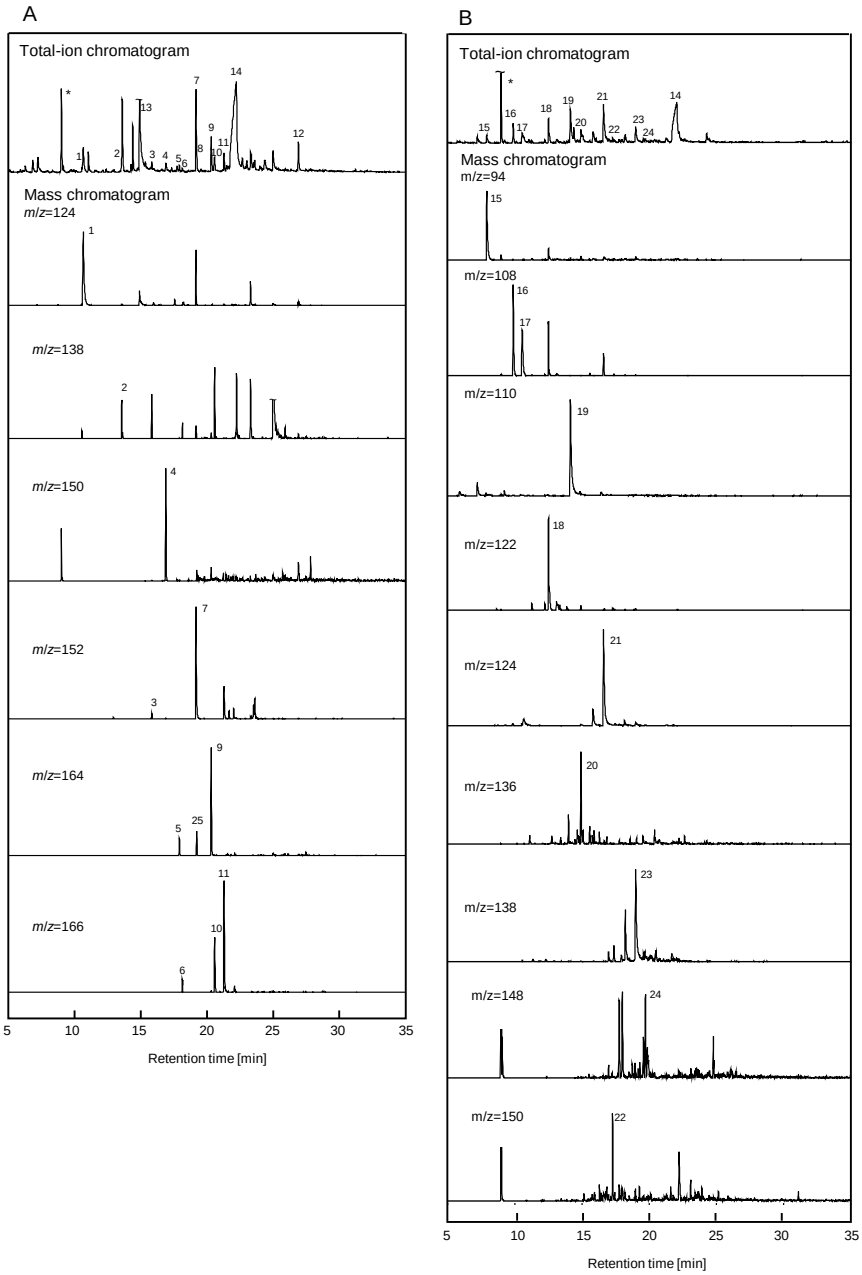

Fig. 2 Total-ion chromatograms and mass chromatograms measured for MeOH-soluble potions obtained in co-pyrolysis of cellulose and lignin (2:1, w/w) (Type A reactor, N_2/ 600 °C).
A: 40 s, B: 80 s.

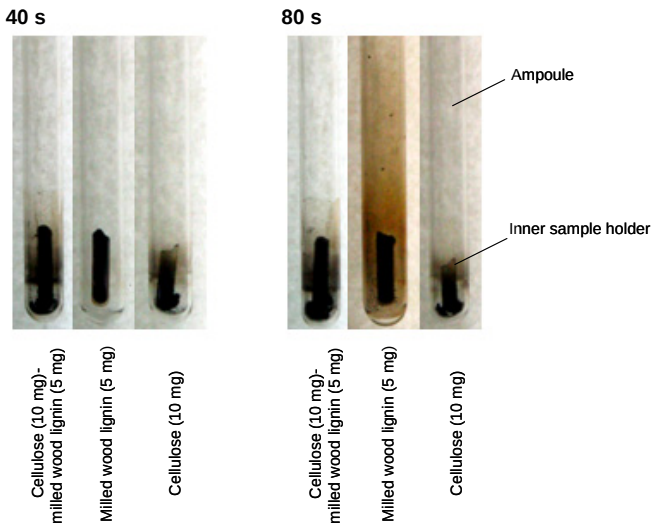

Fig. 3 Ampoules after pyrolysis and tar extraction (Type A reactor).

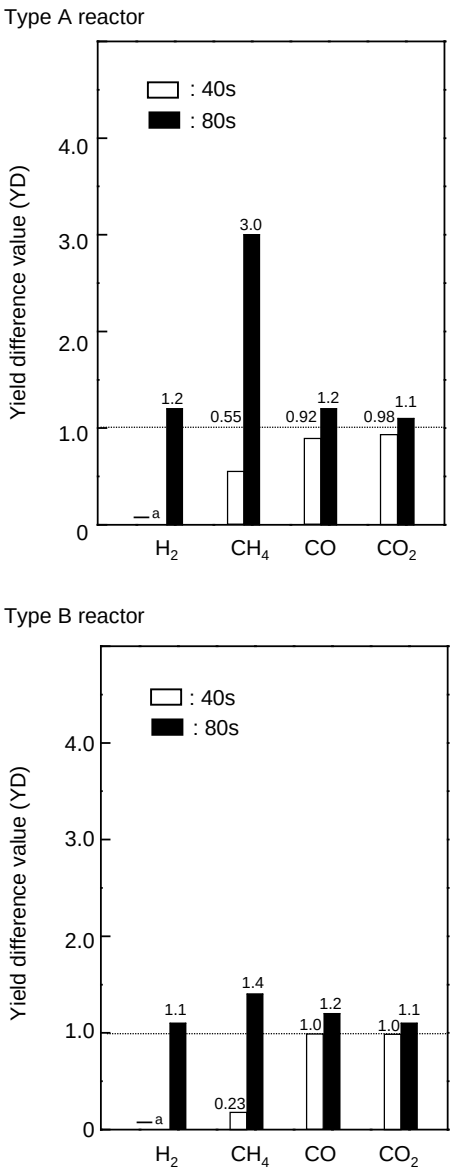

Fig. 4 Yield difference values (YDs) (YD: experimental yield/ estimated yield) obtained for the gaseous products in co-pyrolysis of cellulose and lignin (2:1, w/w) (N_2/ 600 ^oC).
[a] Hydrogen was not detected at 40s.

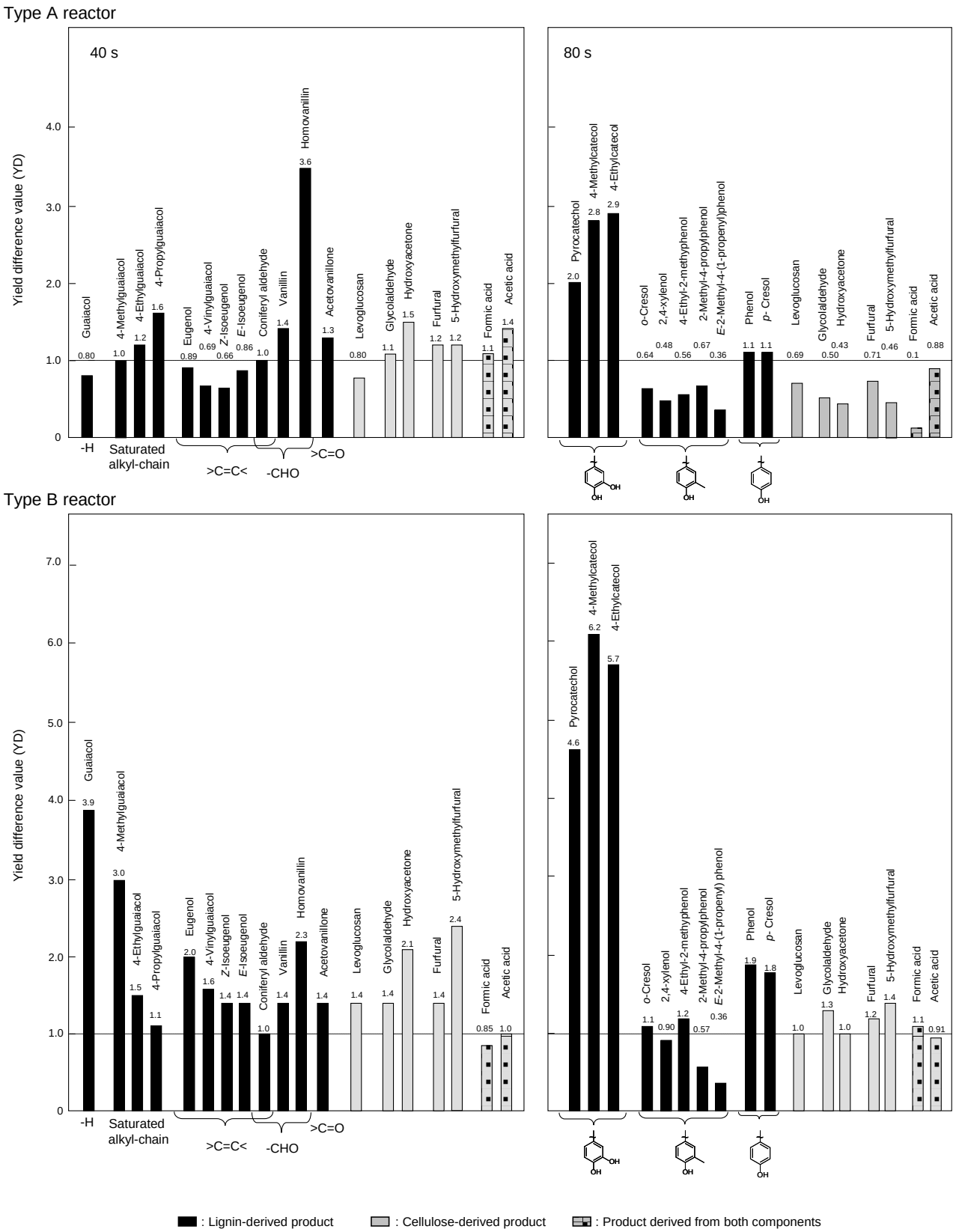

Fig. 5 Yield difference values (YDs) (YD: experimental yield/ estimated yield) obtained for the low MW compounds identified from the tar fractions in co-pyrolysis of cellulose and lignin (2:1, w/w) (N_2/ 600 ^oC).

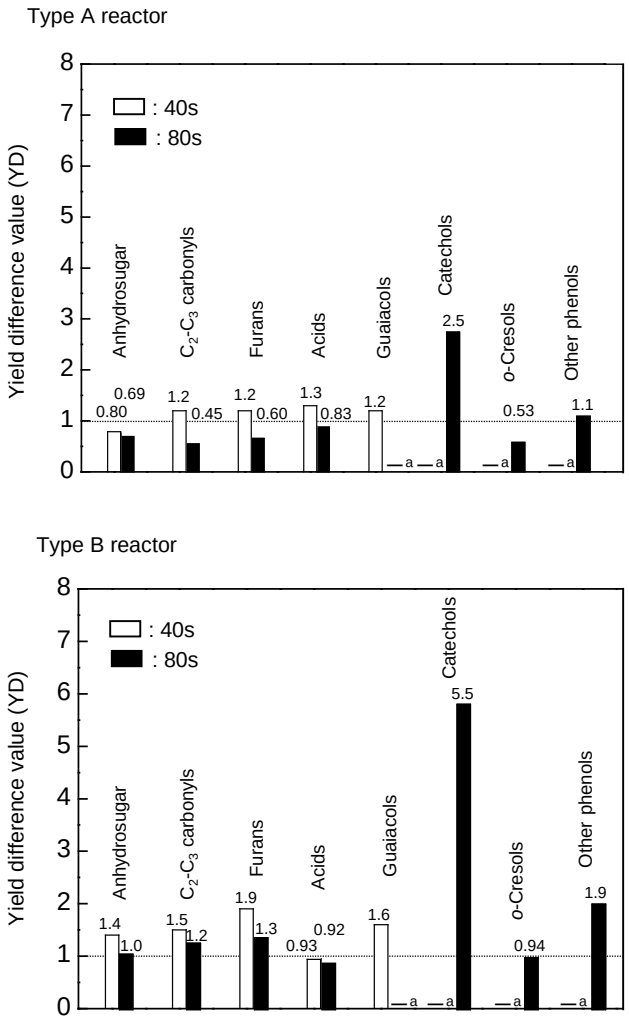

Fig. 6 Yield difference values (YDs) (YD: experimental yield/ estimated yield) of the types of the products in co-pyrolysis of cellulose and lignin (2:1, w/w) (N_2/ 600 ^oC).

[a] Not detected.

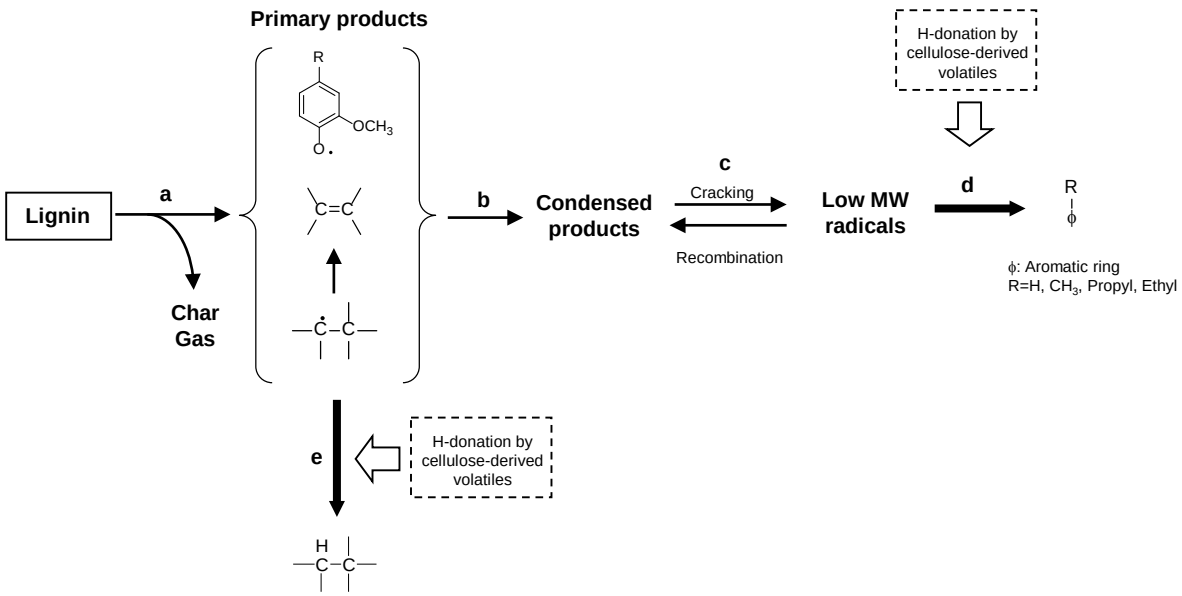

Fig.7 A proposed mechanism for the influences of the cellulose-derived products on the tar formation from lignin.
Bold arrows: enhanced by the cellulose-derived products.

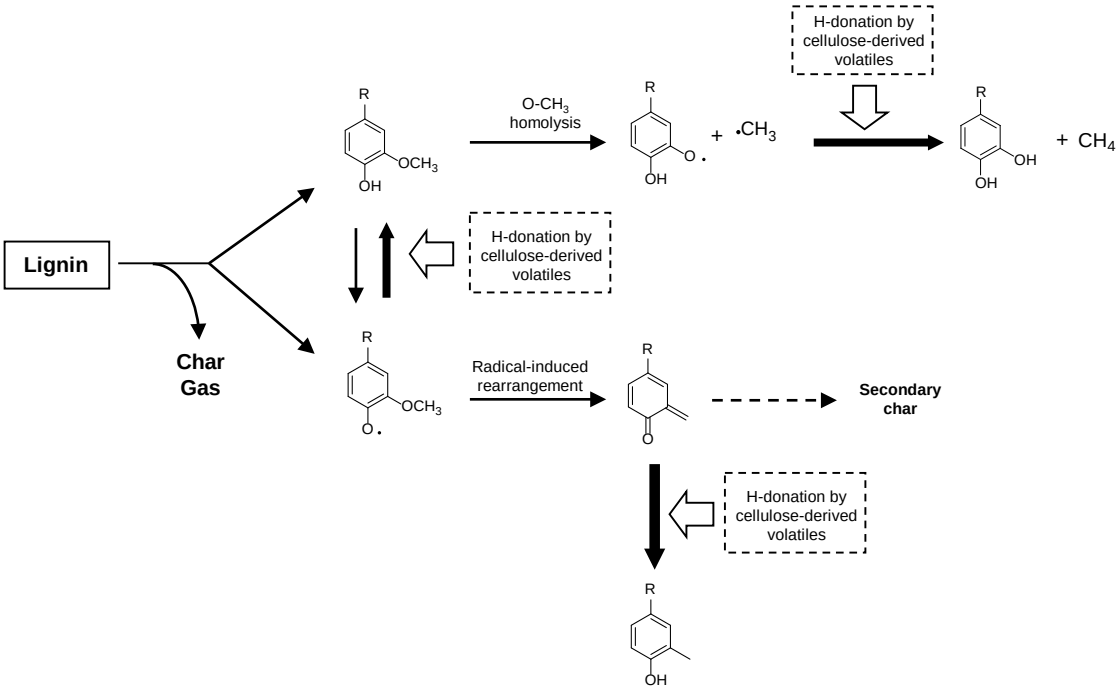

Fig.8 A proposed mechanism for the influences of the cellulose-derived products on the aromatic composition (catechols / *o*-cresols) and the secondary char formation in lignin pyrolysis.
Bold arrows: enhanced by the cellulose-derived products.

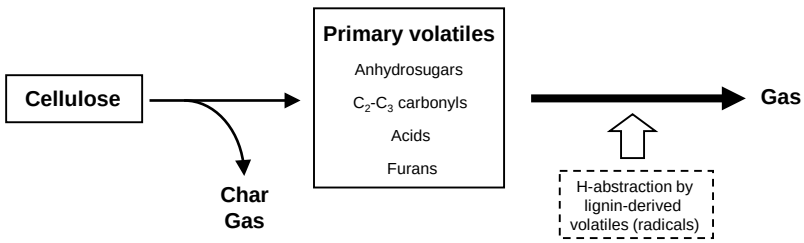

Fig.9 A proposed mechanism for acceleration of the cellulose gasification by the lignin-derived products.
Bold arrow: enhanced by the lignin-derived products.